Ternary Phase Diagram of β-Sitosterol–γ-Oryzanol–Canola Oil

F. M. AlHasawi & M. A. Rogers

Journal of the American Oil Chemists' Society

ISSN 0003-021X
Volume 90
Number 10

J Am Oil Chem Soc (2013) 90:1533-1540
DOI 10.1007/s11746-013-2302-4

Springer

J Am Oil Chem Soc (2013) 90:1533–1540
DOI 10.1007/s11746-013-2302-4

ORIGINAL PAPER

Ternary Phase Diagram of β-Sitosterol–γ-Oryzanol–Canola Oil

F. M. AlHasawi · M. A. Rogers

Received: 27 February 2013 / Revised: 1 July 2013 / Accepted: 10 July 2013 / Published online: 31 July 2013

Abstract β-Sitosterol and γ-oryzanol have been shown to form unique structures in canola oil that have the potential to act as saturated and *trans* fat replacers [1–7]. The ternary phase, reported herein, illustrates numerous interesting physical systems. At high canola oil ratios with low β-sitosterol and γ-oryzanol concentrations, the system has a crystal structure capable of mimicking fat crystal networks. Four mesophases are identified based on Bragg's ratios using small angle X-ray scattering. Two mesophases are lamellar crystals, one is the cubic P phase, and the fourth is an amorphous material due to the low solids content. Wide-angle X-ray further subcategorized the phases based on polymorphic divisions of the hydrocarbon side chain packing. In all, six distinct phases are reported, ranging from lamellar crystals, to liquid crystals to what appears to be a lipid glass.

Keywords Structure · Functional properties · Food and feed science · Nutrition and health · Fat crystallization · Lipid chemistry · Lipid analysis

Introduction

Biomaterials, found in nature, frequently self-assemble, molecule-by-molecule, resulting in the formation of novel supramolecular architectures stabilized by weak, non-covalent interactions [8]. Functionalized biomaterials found in nature, formed via self-assembly, have an array of novel, beneficial functionalities (i.e., silk [9], collagen [10], and tubulin [11]) as well as detrimental architectures that lead to disease (i.e., prion proteins and atherosclerotic plaques[12]). An understanding of these self-assembled supramolecular architectures allows for the future exploitation of nature to develop novel synthetic materials with unique functionalities as well as possible treatments for diseases arising from these adverse architectures.

Numerous foods attain their desirable texture via the crystallization of hardstock triacylglycerides which include the saturated and *trans* fats [13]. Elevated levels of saturated and *trans* fats render them heart unhealthy due to their pronounced contribution towards development of cardiovascular disease [14–17]. *Trans* fats have been associated with an increase in low-density lipoprotein levels (LDL) and a decrease in high-density lipoprotein levels (HDL), while saturated fats have been associated with an increase in LDL levels [17]. Accordingly, a detailed understanding of structurants in lipid phases is essential to deliver alternative technologies to saturated and *trans* hardstock fats [14].

Early work by Bot and Agterof investigated mixtures of γ-oryzanol and phytosterols (including cholesterol and β-sitosterol) to act as a structuring agent in edible liquid oil phases such as sunflower oil [2]. Numerous phytosterols and/or cholesterols mixed in appropriate ratios with γ-oryzanol act as low molecular weight organogelators [2–4, 7, 14, 17]. These mixed systems are capable of trapping oil via capillary action between the self-assembled γ-oryzanol and β-sitosterol co-crystals [17].

The ability of γ-oryzanol and different phytosterols, including β-sitosterol, to co-crystallize results in the formation of hollow tubules that are ~10.9 nm in diameter and just over 1.5 nm wall thickness [14, 18]. Under certain

F. M. AlHasawi · M. A. Rogers (✉)
Department of Food Science, School of Environmental and Biological Sciences, Rutgers University, The State University of New Jersey, New Brunswick, NJ 08901, USA
e-mail: rogers@aesop.rutgers.edu

conditions, these compounds may co-assemble establishing a continuous three-dimensional network capable of immobilizing apolar solvents over macroscopic length scales [2, 3]. Fiber formation occurs when a synergistic interaction occurs between γ-oryzanol and a phytosterol. Individually, neither γ-oryzanol nor phytosterols are capable of effectively immobilizing the oil phase[2].

Co-crystallization of γ-oryzanol and β-sitosterol has made this system of interest to the food industry. The major advantage of this system is that the structurants are generally recognized as safe (GRAS) because γ-oryzanol is found naturally in rice bran oil and β-sitosterol is found in various edible oils [2]. γ-Oryzanol and cholesterol complexes have the potential to reduce cholesterol absorption [6]. Reduction of elevated cholesterol levels is essential as it is linked to 4.5 % of the global mortality rate [19]. γ-Oryzanol also has other health benefits such as inhibiting platelet aggregation and antioxidant properties [20].

Studies on this system have been limited to ratios of γ-oryzanol (Fig. 1b) and β-sitosterol (Fig. 1a) close to 1:1 and at low solids content [2]. Hence, there is limited knowledge on the effect of varying concentrations of these components. In this work, a complete ternary phase has been constructed to examine the full scope of this system at all possible concentration combinations (at 10 wt% increments) using canola oil as the liquid oil phase.

Materials and Methods

Materials and Sample Preparation

Canola oil was obtained from Con Agra Foods, Inc. (Ohama, NE, USA). γ-Oryzanol was obtained from Tsuno Rice Fine Chemicals (Wakayama, Japan). Nitrogen flushed β-sitosterol was obtained from Acros Organics (New Jersey, USA). Canola oil, γ-oryzanol, and β-sitosterol were mixed in varying ratios in 25-ml vials corresponding to each of the points shown in the ternary phase diagram for a total of 66 combinations (Fig. 2). After samples were mixed in their appropriate ratios they were melted at 250 °C and stored at −10 °C until further analysis.

Microscopy Sample Preparation

Samples were melted in a VWR Gravity Convection Oven (VWR International, Radnor, PA, USA) at 250 °C until they reached a liquid state. A drop of the sample was placed on a 3″ × 1″ × 1 mm glass slide. A 24 × 60 mm glass cover slip was placed on top of the sample drop and compressed. Prepared slides were stored at 30 °C for 24 h before acquiring the micrograph.

A Nikon Eclipse microscope (Model No. TE2000-U, Cedar Knolls, NJ, USA) was used for both brightfield and polarized light microscopy under 10× magnification. Brightfield and polarized light micrographs were taken in

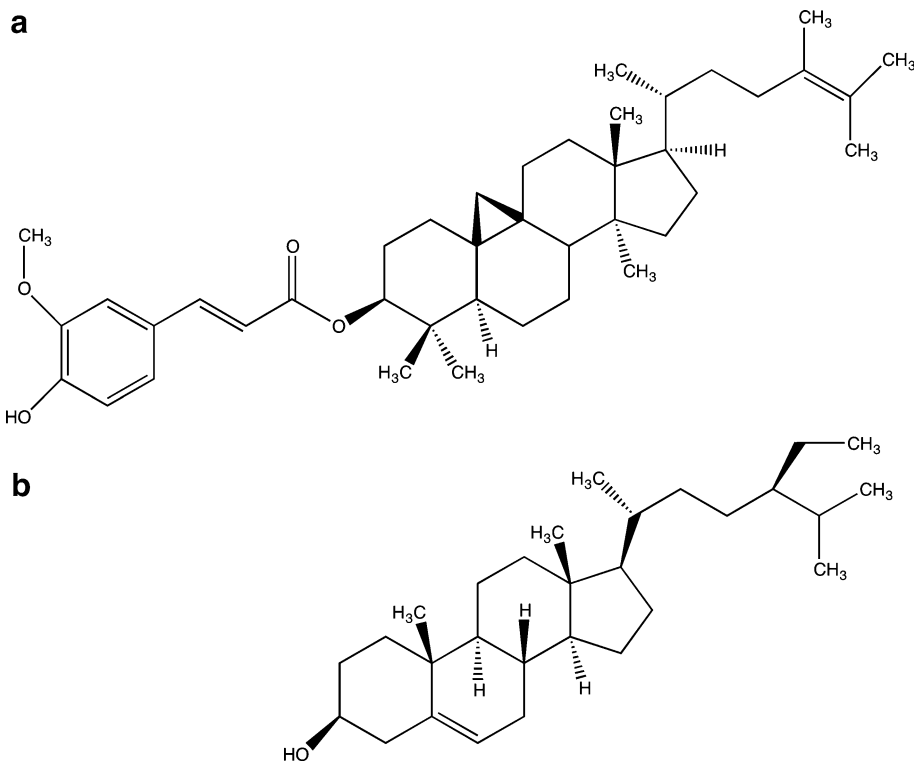

Fig. 1 Chemical structure of **a** β-sitosterol and **b** γ-oryzanol

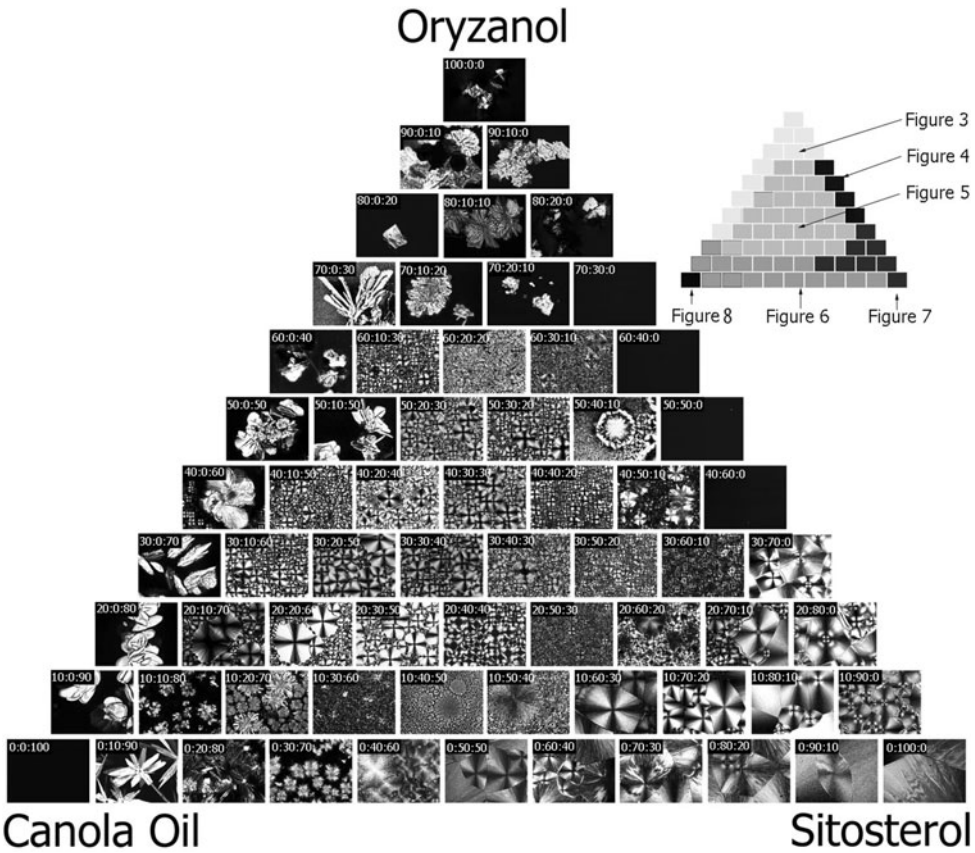

Fig. 2 Ternary phase diagram (TPD) consisting of microscopy images for each tested sample. Grey scale groupings are based on similarities in polymorphic d-spacing patterns. The composition of each point, in the upper right corner of each micrograph, is expressed as the γ-oryzanol:β-sitosterol:canola oil ratios. Inset outlines the borders of the different regions of the ternary phase diagram and the corresponding figure which describes the physical characterization

triplicate. Image analysis was carried out using Image J© software (National Institute of Health, USA) to count the number of crystals per 83 × 64 μm^2 area and to measure the crystal diameter. The longest axis of 10 randomly selected crystals per image area was measured.

Fourier Transform-InfraRed (FTIR)

A Nicolet Fourier Transform-InfraRed spectrometer (Thermo Electron Corporation, Madison, WI, USA) was used to collect interferograms which were obtained from an average of 256 scans. Samples were stored at ~25 °C for 24 h before analysis. Peaks between 3,000 and 3,800 cm^{-1} were analyzed to determine the chemical state of the hydroxyl groups. A broad peak between 3,000 and 3,550 cm^{-1} was indicative of non-specific hydrogen bonding while a sharp peak at ~3,450 cm^{-1} indicated the presence of a highly specific hydroxyl–hydroxyl interaction or the presence of a free hydroxyl group [6, 7, 21].

Differential Scanning Calorimetry (DSC) Sample Preparation

Samples ranging from 3 to 6 mg were sealed in Qseries T-zero Aluminum pans and lids (TA Instruments -Waters, LLS, New Castle, Delaware, USA). Filled pans were stored at ~25 °C for 24 h before analysis. The DSC chamber was pre-flushed with nitrogen (0.5 ml/min) while the samples were heated at 5 °C/min to 200 °C and held at 200 °C for 10 min. The samples were then cooled at 5 °C/min to 10 °C and held for 10 min. TA Universal Analysis 2000 Software (TA Instruments—Waters, LLC, Delaware, USA) was used to determine crystallization and melting temperatures, as well as glass transition temperature by integrating the peak using a tangential baseline.

X-ray Diffraction

A Rigaku Multiplex Powder X-ray Diffractometer (Rigaku, Japan) with a ½ degree scatter slit, a ½ degree divergence slit, and a 0.3 mm receiving slit, was set at 40 kV and 44 mA to determine the polymorphic form of the different combinations in the various samples. Scans were performed from 1 to 30° 2 theta (θ) at 0.2°/min. Small angle X-ray scattering (SAXS) was used to determine mesophases within TPD based on Bragg's ratio values previously obtained [22]. Wide-angle X-ray scattering (WAXS) was used to further subcategorize the regions based on polymorphic behavior; as per similarities in d-spacing patterns.

Discussion

Using the Bragg's ratios obtained from the small angle X-ray diffraction [22] and wide-angle X-ray scattering to further sub-categorize the phases based on the polymorphic form present a total of six different phases were observed (Fig. 2). Similarities in melting and crystallization temperatures, FT-IR spectral peaks between 3,000 and 3,800 cm^{-1}, and morphological characteristics were also utilized to categorize the TPD regions.

γ-Oryzanol ratios between 30 to 100 %, combined with low β-sitosterol ratios (i.e., 0–20 %) and the concentration of canola oil between 70 and 0 % generated a mixed crystalline phase (Fig. 3). The characteristic melting temperatures were 100 and 125 °C; and a single crystallization peak at 50 °C was observed (Figs. 3a, b). In this region of the TPD, a large degree of supercooling (~50 °C) is required to initiate crystallization. Upon heating, a much more complex transition (Fig. 3a) is observed suggesting that during crystallization, an unstable polymorphic form nucleates from the melt. As the sample melts, there is an increase in the molecular mobility allowing the sample to recrystallize into a more stable polymorph at 110 °C, which then melts at 125 °C. The Bragg's ratio of the small angle X-ray scattering diffraction peaks (i.e. 001 ≈ 42 Å, 002 ≈ 20 Å, 003 ≈ 13 Å and 004 ≈ 9.5 Å) indicates a lamellar mesophase (Fig. 3c) [22]. This region of the TPD contains lamellar crystals with a wide-angle spacing observed at 5.5, 5, and 3.6 Å (Fig. 3d). The broad peak observed in the FT-IR spectra between 3,000 and 3,550 cm^{-1} is indicative of non-specific hydrogen bonding of pure γ-oryzanol in the absence of β-sitosterol (Fig. 3e) [6, 7, 21]. These lamellar crystals have a spherulitic morphology (Fig. 3f) and are 0.06 ± 0.03 μm in diameter and ~46 crystals are present per 5,588 μm^2. Since the degree of supercooling was large, it is expected that rapid nucleation will result in a large number of crystals. The rapid initial nucleation provides a large surface area for crystal growth, which results in crystals with a small diameter.

The second distinct region of the TPD was at γ-oryzanol ratios between 40 and 70 % combined with 60–30 % β-sitosterol and no canola oil (Fig. 4). Interestingly, upon cooling no exothermic peak was observed associated with a clear phase transition (Fig. 4b). However, a shift in the baseline at 30 °C, indicative of a glass transition, was observed [23]. The shift in the baseline is also present in the melt (Fig. 4a) at approximately 40 °C. It is important to note that slow cooling rates, at 0.1 °C/min, and a 24 h hold were done to observe if the lack of a crystallization peak was due to an insufficiently short experimental time frame. However, neither had an effect on the position of the baseline shift nor the appearance of an exothermic crystallization peak. Following the baseline shift, during heating, an exothermic crystallization (~80 °C) and endothermic melt (~130 °C) are observed (Fig. 4b). Along with the lack of a discernable exothermic peak, there is no sharp peak at 3,450 cm^{-1} (Fig. 4e), suggesting there is no highly specific intermolecular interactions between γ-oryzanol and β-sitosterol [6, 7, 21]. A sharp X-ray diffraction peak is observed at 40 Å, followed by a broad peak; the broadness of this peak proves allocating a specific d-spacing value to be difficult. Accordingly, allocating a mesophase to this region is not possible although it is likely to be a nematic-like liquid crystal (Fig. 4c). In the wide-angle region only a very diffuse single amorphous peak is present illustrating that there is no sub cell contained in this material (Fig. 4d, e) [6, 7, 21]. Polarized light micrographs were unable to detect any birefringence lending credence to the hypothesis that this complex material may form a glass-like material, with some level of order (however the form of order cannot be determined at this time, as discussed above—Fig. 4c) in this region of the TPD (Fig. 4f). There is precedence for mixed cholesterol systems to structure in these glass-forming liquid-crystals [24].

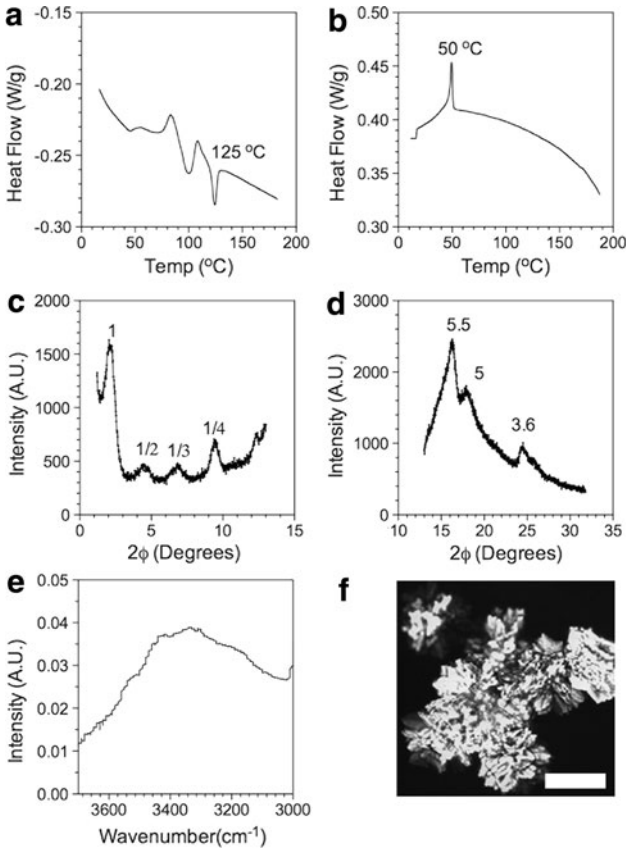

Fig. 3 High γ-oryzanol (70–100 %) combined with low β-sitosterol composition (20–0 %) and with canola oil (0–70 %), respectively.**a** DSC heating thermogram, **b** DSC cooling thermogram, **c** small angle X-ray diffraction, **d** wide angle X-ray diffraction (Å), **e** FT-IR spectrum, **f** microscopy imaging (scale bar = 100 μm)

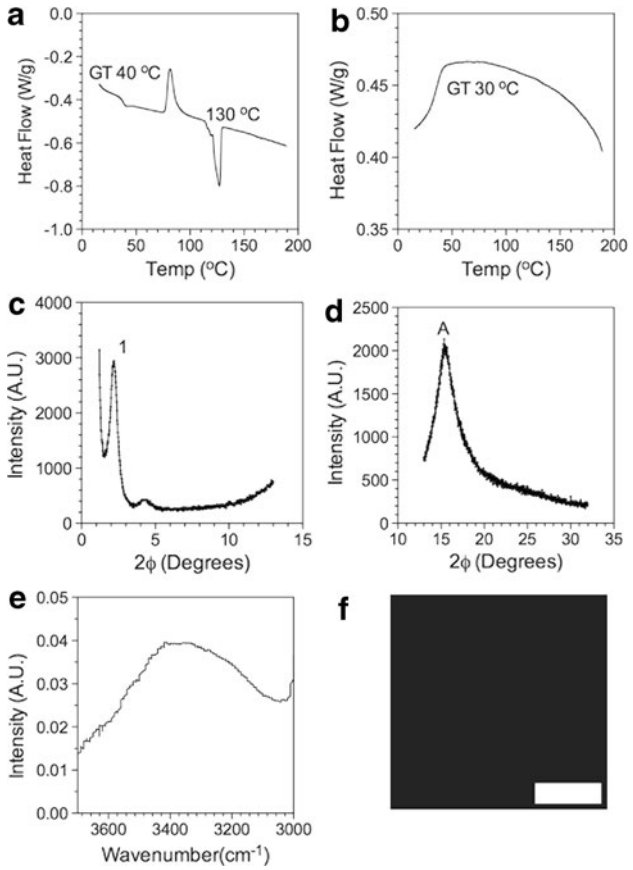

Fig. 4 (40–70 %) γ-oryzanol combined with (60–30 %) β-sitosterol, respectively; in the absence of canola oil (0 %). **a** DSC heating thermogram, **b** DSC cooling thermogram, **c** small angle X-ray diffraction, **d** wide angle X-ray diffraction (Å), **e** FT-IR spectrum, **f** microscopy imaging (scale bar = 100 μm)

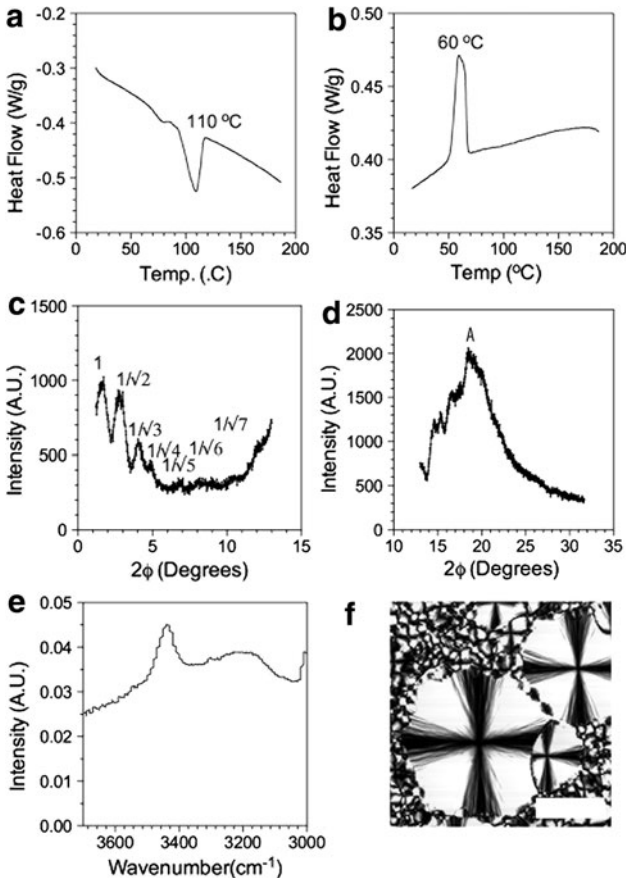

Fig. 5 (20–70 %) γ-oryzanol combined with (60–10 %) β-sitosterol and (20–60 %) canola oil, respectively. **a** DSC heating thermogram, **b** DSC cooling thermogram, **c** small angle X-ray diffraction, **d** wide angle X-ray diffraction(Å), **e** FT-IR spectrum, **f** microscopy imaging (scale bar = 100 μm)

The central region of the TPD forms a single phase from 20 to 70 % γ-oryzanol, 60 to 10 % β-sitosterol and 20 to 60 % canola oil (Fig. 5). The characteristic melting temperature for this region is 120 °C (Fig. 5a) and the crystallization temperature is 60 °C (Fig. 5b). Although the transition temperatures have decreased by 10 °C compared to the lamellar phase previously described (Figs. 3a, b), the degree of supercooling to induce nucleation remains constant at 50 °C. The Bragg's ratio, observed in short-angle X-ray scattering (i.e. 001 ≈ 50 Å, 002 ≈ 30 Å, 003 ≈ 22 Å, 004 ≈ 17 Å, 005 ≈ 12 Å, 006 ≈ 9 Å, and 007 ≈ 7 Å), indicates a cubic P mesophase (Fig. 5c) [22]. The wide-angle X-ray scattering (Fig. 4d) indicates a single amorphous peak. From the ratios of γ-oryzanol and β-sitosterol in this region it is evident that a mixed crystalline phase of the two components occurs. The broad peak observed on the FT-IR spectrum between 3,000 and 3,400 cm^{-1} is indicative of the hydroxyl groups being involved in non-specific hydrogen bonding; while the sharp peak at 3,450 cm^{-1} indicates highly specific hydroxyl–hydroxyl interaction or the presence of free hydroxyl groups not involved in hydrogen bonding [6, 7, 21]. Polarized light micrographs showed a cross morphology for this region of the TPD; which is a typical characteristic of liquid crystals. Further, due to the anisotropic nature of liquid crystals, polarized light micrographs show typical birefringence for the cubic mesophase (Fig. 5f). Although the image was acquired in grey scale, when observed under polarized light, a typical colored pattern was observed. The average size of the liquid crystals is 0.17 ± 0.05 μm, with 67 crystals per 5,588 μm. Similar to the lamellar phase described in Fig. 3, the large number of crystals is observed to be associated with the high degree of supercooling (50 °C) and associated rapid degree of supercooling.

At low γ-oryzanol ratios (i.e., 0–20 %), combined with varying ratios of β-sitosterol (90–10 %) and canola oil (10–90 %), a single phase is formed at the base of TPD (Fig. 6). This material melts at 130 °C (Fig. 6a) and crystallizes at 100 °C (Fig. 6b) with an average supercooling of

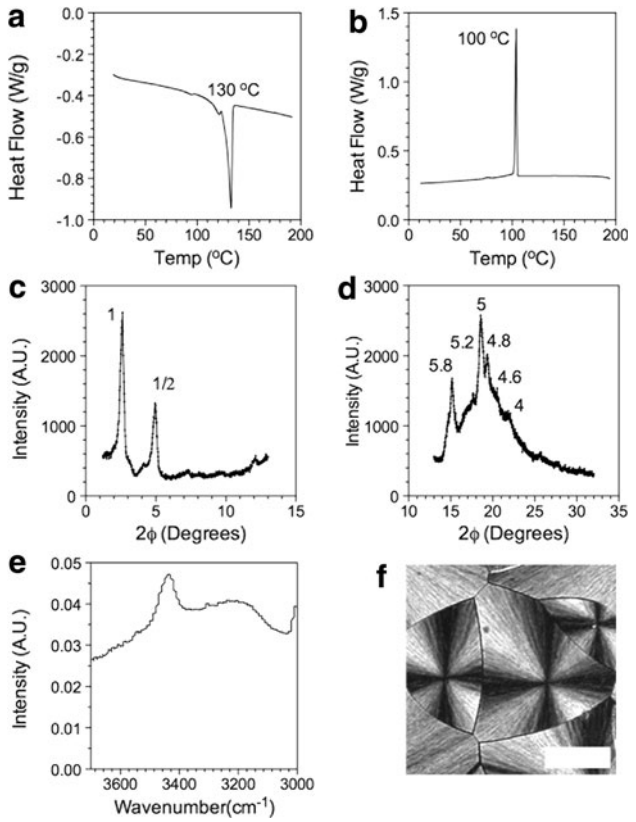

Fig. 6 (20–0 %) γ-oryzanol combined with (0–90 %) β-sitosterol and (0–90 % canola oil), respectively. **a** DSC heating thermogram, **b** DSC cooling thermogram, **c** small angle X-ray diffraction, **d** wide angle X-ray diffraction (Å), **e** FT-IR spectrum, **f** microscopy imaging (scale bar = 100 μm)

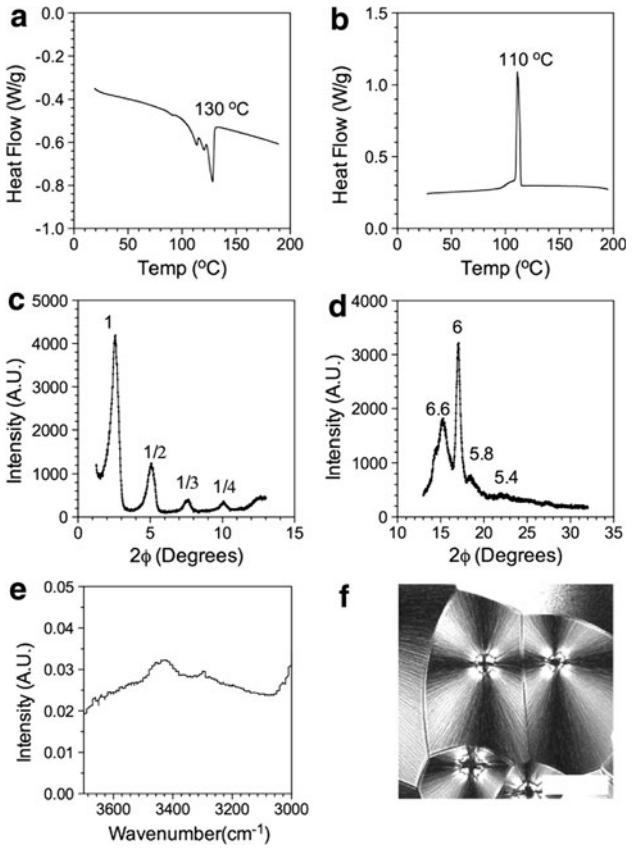

Fig. 7 (0–30 %) γ-oryzanol combined with (100–70 %) β-sitosterol and (0–30 %) canola oil, respectively. **a** DSC heating thermogram, **b** DSC cooling thermogram, **c** small angle X-ray diffraction, **d** wide angle X-ray diffraction (Å), **e** FT-IR spectrum, **f** microscopy imaging (scale bar = 100 μm)

30 °C. A lamellar mesophase with Bragg's ratios in small angle spacing at 001 ~ 33 Å and 002 ~ 18 Å (Fig. 6c) is observed; while a different sub cell was observed (5.8, 5.2, 5, 4.8, 4.6, and 4 Å) (Fig. 6d). The FT-IR spectra of this region shows both a very distinct broad peak between 3,000 and 3,400 cm^{-1} and a sharp peak at around 3,450 cm^{-1} (Fig. 6e). This corresponds to involvement of non-specific hydrogen bonding and free hydroxyl groups in the monomeric form or of highly specific hydroxyl–hydroxyl interaction, respectively [6, 7, 21]. A mixture of lamellar crystals is visible in this region (Fig. 2). Average diameter of the crystals is 0.09 ± 0.2 μm; 23 crystals are found on average per 5,588 μm^2. Compared to the two previously discussed regions of TPD (described in Figs. 3 and 5); fewer crystals are present which is most likely attributed to the reduction in the degree of supercooling (~30 °C).

Low γ-oryzanol (0–30 %) ratios combined with high (100–70 %) β-sitosterol ratios and low canola oil ratios (0–30 %), respectively, forms a phase in the bottom right corner of TDP (Fig. 7). This region has a melting temperature of 130 °C and a crystallization temperature of 110 °C (Fig. 7a, b), with a supercooling of only 20 °C suggesting that less energy is required to induce nucleation. A lamellar structure is present as evidenced by the small angle spacings (i.e. 001 ≈ 33 Å, 002 ≈ 17 Å, 003 ≈ 12 Å, and 004 ≈ 9 Å), in Fig. 7c [22]. Wide-angle d-spacings are observed at 5.8, 5.2, 5, 4.8, 4.6, and 4 Å (Fig. 7d). A broad peak between 3,000 and 3,400 cm^{-1} followed by a sharp peak at 3,450 cm^{-1} was observed (Fig. 7e). As shown in Fig. 7f, the Maltese cross morphology is characteristic of this phase; however, when observed under polarized light, no colored pattern was evident. The average diameter of the crystals is 0.11 ± 0.04 μm; while 14 crystals are present per 5,588 μm^2. Compared to all other regions of TPD, this region of TPD contains the lowest number of crystals in the given area and simultaneously, the lowest degree of supercooling (20 °C).

Figure 8 illustrates a region composed of a single unit located in the far left corner of TPD. Its ratio composition is 100 canola: 0 γ-oryzanol: 0 β-sitosterol. The lack of solid material is illustrated in the inability

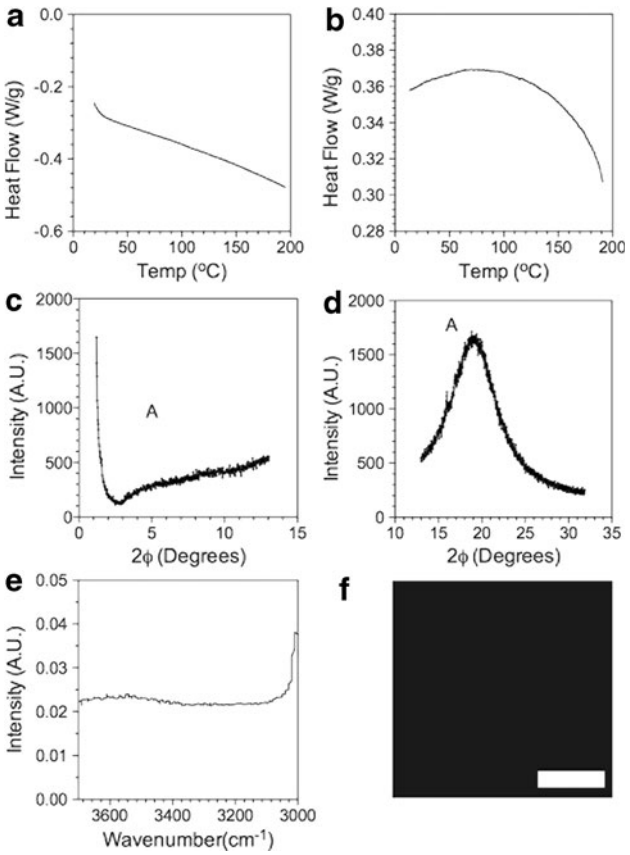

Fig. 8 0 % γ-oryzanol, 0 % β-sitosterol, and 100 % canola oil. **a** DSC heating thermogram, **b** DSC cooling thermogram, **c** small angle X-ray diffraction, **d** wide angle X-ray diffraction (Å), **e** FT-IR spectrum, **f** microscopy imaging (scale bar = 100 μm)

to detect any data in all analyses conducted (Fig. 8). As a result of the absence of solids, neither an endothermic melt nor exothermic crystallization are detected (Fig. 8a, b). The presence of 100 % canola oil resulted in a lack of small angle or wide angle X-ray scattering (Fig. 8c, d). Polarized light micrographs were unable to detect any birefringence again due to absence of solid material (Fig. 8f).

It is clear from the different regions of the ternary phase diagram that numerous materials result by modifying the amount of γ-oryzanol, β-sitosterol and canola oil. Structures range from fibrillar self-assembled molecular gels capable of immobilizing oil at very low concentration confirming previous work done on this system [2–4, 6, 7, 18]. As the concentration of a single phase increases, spherulitic crystals result and when the concentration of both phases increases liquid crystals form. Finally, at 100 % solids combined at near 1:1 ratios of γ-oryzanol and β-sitosterol an amorphous material results, which is a very unique material and it behaves as a lipid "glass-like" material.

Conclusions

β-Sitosterol and γ-oryzanol form unique structures in canola oil that have the potential to act as saturated and *trans* fat replacers at low solids contents [1–7]. The ternary phase, reported herein, illustrates numerous interesting physical systems, which may have applications beyond saturated and *trans* fat replacers. At high canola oil ratios with low β-sitosterol and γ-oryzanol concentrations, the system has a crystal structure capable of mimicking fat crystal networks. Six distinct phases were identified ranging from lamellar crystals, to liquid crystals to what appears to be a lipid glass [25].

References

1. Akiyama Y et al (2005) Free radical scavenging activities of γ-oryzanol constituents. Food Sci Technol Res 11:295–297
2. Bot A, Agterof WGM (2006) Structuring of edible oils by mixtures of γ-oryzanol with β-sitosterol or related phytosterols. J Am Oil Chem Soc 83:513–521
3. Bot A, den Adel R, Roijers EC (2008) Fibrils of gamma-oryzanol plus beta-sitosterol in edible oil organogels. J Am Oil Chem Soc 85(12):1127–1134
4. Bot A et al (2009) Non-TAG structuring of edible oils and emulsions. Food Hydrocoll 23(4):1184–1189
5. Rogers MA (2009) Novel structuring strategies for unsaturated fats—meeting the zero-trans, zero-saturated fat challenge: a review. Food Res Int 42(7):747–753
6. Rogers MA (2011) Co-operative self-assembly of cholesterol and γ-oryzanol composite crystals. CrystEngComm 13:7049–7057. doi:10.1039/C1CE05818E
7. Rogers MA et al (2010) Multicomponent hollow tubules formed using phytosterol and γ-oryzanol-based compounds: an understanding of their molecular embrace. J Phys Chem 114:8278–8295
8. Zhang S (2003) Fabrication of novel biomaterials through molecular self-assembly. Nat Biotechnol 21(10):1171–1178
9. Jin H-H, HKaplan DL (2003) Mechanism of silk processing in insects and spiders. Nature 424:1057–1061
10. Caria A et al (2004) Elastic scattering and light transport in three-dimensional collagen gel constructs: a mathematical model and computer simulation approach. IEEE Trans Nanobiosci 3:85–89
11. Oakley BR, Akkari YN (1999) Tubulin at ten: progress and prospects. Cell Struct Funct 24:365–372
12. Liu W, Prausnitz JM, Blanch HW (2004) Amyloid fibril formation by peptide LYS (11-36) in aqueous trifluoroethanol. Biomacromolecules 5:1818–1823
13. Floter EBA, Williams C, Buttriss J (2006) Developing products with modified fats, in improving the fat content of food. Woodhead Publishing Ltd: Cambridge, UK. p. 411–427
14. Pernetti M et al (2007) Structuring of edible oils by alternatives to crystalline fat. Curr Opin Colloid Interface Sci 12:221–231
15. Keys A, JT A, Grande F (1965) Serum cholesterol response to changes in diet: IV. Particular saturated fatty acids in the diet. Metabolism 14(7):776–787
16. Mensink R et al (2003) Effects of dietary fatty acids and carbohydrates on the ratio of serum total to HDL cholesterol and on serum lipids and apoproteins: a meta analysis of 60 controlled trials. Am J Clin Nutr 77:1146–1155

17. Daniel Co E, Marangoni AG (2012) Organogels: an alternative edible oil-structuring method. J Am Oil Chem Soc 89:749–780
18. Bot A et al (2012) Elucidation of density profile of self-assembled sitosterol + oryzanol tubules with small-angle neutron scattering. Faraday Discuss 158:223–238
19. World Health Organization (2013) Global health observatory: raised cholesterol [cited 2013 08 February]; Available from: http://www.who.int/gho/ncd/risk_factors/cholesterol_text/en/index.html
20. Ismail M et al (2010) Gamma-oryzanol rich fraction regulates the expression of antioxidant and oxidative stress related genes in stressed rat's liver. Nutr Metab 7(23):1–13
21. Lin-Vien D et al (1991) The handbook of infrared and raman characteristic frequencies of organic molecules. Academic Press, London
22. Hyde ST (2001) Identification of lyotropic liquid crystalline mesophases. In: Holmberg K (ed) Handbook of applied surface and colloid chemistry. John Wiley, New York
23. Hohne GWH, Hemminger WF, Flammersheim H-J (2003) Differential scanning calorimetry. Springer-Verlag Berlin, Heidelberg, pp 203–212
24. Tamaoki N et al (2003) Photochemical phase transition and molecular realignment of glass-forming liquid crystals containing cholesterol/azobenzene dimesogenic compounds. Chem Mater 15:719–726
25. Pérez-Martínez D et al (2007) The cooling rate effect on the microstructure and rheological properties of blends of cocoa butter with vegetable oils. Food Res Int 40:47–62